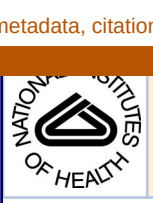

Published in final edited form as:

Mol Cancer Res. 2014 November ; 12(11): 1610–1620. doi:10.1158/1541-7786.MCR-14-0006.

PTEN deficiency mediates a reciprocal response to IGF-1 and mTOR inhibition

Mukund Patel[1,*], **Nicholas C. Gomez**[1,2,*], **Andrew W. McFadden**[1], **Billie M. Moats-Staats**[3], **Sam Wu**[1], **Andres Rojas**[1], **Travis Sapp**[4], **Jeremy M. Simon**[1], **Scott V. Smith**[4], **Kathleen Kaiser-Rogers**[3,4], and **Ian J. Davis**[1,3,5]

[1] Department of Genetics and Lineberger Comprehensive Cancer Center, University of North Carolina at Chapel Hill, Chapel Hill, North Carolina, USA

[2] Curriculum in Genetics and Molecular Biology, University of North Carolina at Chapel Hill, Chapel Hill, North Carolina, USA

[3] Department of Pediatrics, University of North Carolina at Chapel Hill, Chapel Hill, North Carolina, USA

[4] Department of Pathology and Laboratory Medicine, University of North Carolina at Chapel Hill, Chapel Hill, North Carolina, USA

[5] Carolina Center for Genome Sciences, University of North Carolina at Chapel Hill, Chapel Hill, North Carolina, USA

Abstract

Recent evidence implicates the insulin-like growth factor (IGF) pathway in development of Ewing Sarcoma, a highly malignant bone and soft tissue tumor that primarily affects children and young adults. Despite promising results from preclinical studies of therapies that target this pathway, early phase clinical trials have shown that a significant fraction of patients do not benefit, suggesting that cellular factors determine tumor sensitivity. Using FAIRE-seq, a chromosomal deletion of the PTEN locus in a Ewing sarcoma cell line was identified. In primary tumors PTEN deficiency was observed in a large subset of cases, although not mediated by large chromosomal deletions. PTEN loss resulted in hyper-activation of the AKT signaling pathway. PTEN rescue led to decreased proliferation, inhibition of colony formation, and increased apoptosis. Strikingly, PTEN loss decreased sensitivity to IGF-1R inhibitors but increased responsiveness to

Corresponding Author Ian J. Davis, Lineberger Comprehensive Cancer Center, University of North Carolina at Chapel Hill, 450 West Drive, C/B 7295, Chapel Hill, NC, 27599-7295, USA, ijdavis@email.unc.edu 919-966-5360.

*These authors contributed equally to this manuscript.

Current address: Mukund Patel, Gentris Corporation, 133 Southcenter Court, Suite 400, Morrisville, NC, 27560

Disclosure of Potential Conflicts of Interest

No potential conflicts of interest were disclosed.

Authors' Contributions

Conception and design: M. Patel, N. Gomez, I. Davis

Acquisition of data: M. Patel, N. Gomez, A. McFadden, J. Simon, T. Sapp, S. Wu, A. Rojas, S. Smith, B. Moats-Staat

Analysis and interpretation of data: M. Patel, N. Gomez, A. McFadden, J. Simon, T. Sapp, S. Wu, A. Rojas, I. Davis

Writing, review, and/or revision of the manuscript: M. Patel, N. Gomez, I. Davis

Administrative, technical, or material support: M. Patel, N. Gomez, A. McFadden, J. Simon, S. Smith, T. Sapp, A. Rojas, I. Davis, K. Kaiser-Rogers

temsirolimus, a potent mTOR inhibitor, as marked by induction of autophagy. These results suggest that PTEN is lost in a significant fraction of primary tumors and this deficiency may have therapeutic consequences by concurrently attenuating responsiveness to IGF-1R inhibition while increasing activity of mTOR inhibitors. The identification of PTEN status in the tumors of patients with recurrent disease could help guide the selection of therapies.

Keywords

Ewing sarcoma; PTEN; IGF-1; PI3K signaling; temsirolimus; autophagy

Introduction

Ewing sarcoma is a malignant bone and soft tissue tumor primarily affecting children and young adults. Despite intensive chemotherapy, surgery and radiation therapy approximately 50% of patients ultimately succumb to the disease. Ewing sarcoma is characterized by chromosomal translocations that fuse a member of the TET family to one of a subset of ETS transcription factors (1, 2). Eighty to eighty-five percent of Ewing Sarcoma tumors contain t(11;22)(q24;q12) generating an in-frame fusion of *EWSR1* to *FLI1* (2). The resulting chimeric EWS-FLI1 protein is a potent transcriptional modulator that regulates multiple genes implicated in malignant transformation (3, 4).

Several lines of evidence support a role for the insulin-like growth factor (IGF) pathway in the development of Ewing sarcoma. EWS-FLI1 regulates *IGF1* in Ewing sarcoma cell lines and is induced by EWS-FLI1 in mesenchymal stem cells (5-7). IGF-1 and its receptor (IGF-1R) are expressed in tumors, and IGF-1 expression in cell lines leads to autocrine activation (8, 9). IGF-1 signaling is necessary for the survival and proliferation of Ewing sarcoma cells (10, 11), transformation of murine fibroblasts by EWS-FLI (12) as well as for normal bone development (13). The promising results of preclinical trials targeting IGF pathway in Ewing Sarcoma has made it an attractive therapeutic target (14-17). However, studies of IGF-1 and IGF-1R inhibitors in early phase clinical trials have shown a limited response rate (18-20). A biomarker predictive of individuals who may respond to IGF1-mediated treatment remains to be identified (21, 22).

IGF-1 bound to IGF-1R initiates a signaling cascade through the PI3K pathway resulting in phosphorylation of downstream targets including AKT. Phosphorylation of AKT at serine-473 (S473) and threonine-308 (T308) promotes cell cycle progression, cell survival, migration, and metabolism through differential interactions with multiple substrates including mTOR (23, 24). Signaling through the PI3K pathway is attenuated by PTEN through dephosphorylation of PIP_3 (25). The loss of PTEN results in increased accumulation of PIP_3 and AKT activation, which has been associated with poor clinical outcomes (26-28). The loss or mutation of PTEN has been demonstrated in a range of cancers (26-30); however, the function of PTEN in Ewing sarcoma has yet to be investigated.

Here we describe PTEN loss in Ewing sarcoma and its consequences on IGF and mTOR signaling, as well as on biochemical responses to small molecule inhibitors. PTEN deficiency augments PI3K signaling to AKT while diminishing cellular responsiveness to

IGF inhibition. Interestingly, PTEN loss enhances sensitivity to autophagy induced by mTOR inhibition. Together these data suggest how PTEN loss may influence the response to biological therapies in Ewing sarcoma.

Materials and Methods

Fluorescent *In Situ* Hybridization

The RP11-383D9 (D9) and RP11-846G17 (G17) BACs were obtained from the Children's Hospital Oakland Research Institute. Bacterial cultures of both BACs were grown in LB with 25 μg/mL chloramphenicol and DNA extracted using Qiagen Plasmid Midi Kit with slight modifications (10 mL of Buffer P1, P2, and P3 and DNA was eluted in 1 mL increments using prewarmed Buffer QF at 65 °C). Probes were made using 1 μg of BAC DNA by nick translation (Abbott Laboratories, cat #32-801300) with Red-dUTP (Abbott, cat # 02N34-050) according to manufacturer's protocol. A Chromosome 10 centromeric probe (CEP, Abbott Laboratories) was used as a control. Cell lines were trypsinized, washed, and then resuspended in a small volume of PBS. 10 mL of KCl at 37 °C was added dropwise with gentle agitation for the first 2 mL. After adding KCl, the solution was mixed and placed in a 37 °C water bath for 12 min after which 1 mL of fresh cold 3:1 methanol:acetic acid (fixative) was added. Cells were collected by centrifugation (10 min, 1000 RPM) and the pellet was resuspended in 10 mL of fresh cold fixative which was added dropwise with gentle agitation for the first 2 mL and incubated at room temperature for 10 min. This process was repeated twice. BAC and CEP probes were then hybridized to each cell line before imaging. PTEN and CEP signals were manually counted from at least 20 nuclei in five separate fields.

Cell culture and Antibodies

Unless otherwise indicated, EWS502, EWS894, and RD-ES cell lines were cultured in RPMI supplemented with 15% fetal bovine serum. A673 and MHH-ES-1 cell lines were cultured in RPMI supplemented with 10% fetal bovine serum. SK-ES cells were cultured in McCoy's 5A supplemented with 15% fetal bovine serum. SK-N-MC cells were cultured in DMEM supplemented with 10% fetal bovine serum, 2 mM L-glutamine and 1X nonessential amino acids. EWS502 and EWS894 were kindly provided by Dr. Jonathan Fletcher (Brigham and Women's Hospital, Boston) and A673 by Dr. Stephen Lessnick (Univ. of Utah). Other cell lines were obtained from the DSMZ (Braunschweig, Germany). HUVEC cells (Lifeline Technologies) were cultured in Vasculife Basal Media (Lifeline Technologies) supplemented with 10% FBS. CD99 (clone 12E7, Ready-to-use, PA0559, Leica Microsystems) and PTEN antibodies (clone 138G6, 9559S, Cell Signaling Technology) were used for IHC and IF. AKT (#4691), pAKT T308 (#2965), pAKT S473 (#4060) and LC3B (#3868), cleaved PARP (#5625) were used for immunoblotting (Cell Signaling Technology).

Cell Proliferation, Apoptosis, Soft agar, and Autophagy

pLL5.0-PTEN (which expresses PTEN), pLL5.0-shPTEN (which expresses an shRNA directed at PTEN 5'-GTATAGAGCGTGCAGATAG-3') and pLL5.0-shNS (which expresses a non-specific shRNA as a control) were kindly provided by Dr. James Bear

(UNC-Chapel Hill). Lentivirus was produced as previously described (31). EWS502 cells were transduced with either pLL5.0-PTEN or vector control lentivirus in the presence of polybrene (6 μg/mL) for 3 hours, after which media was changed and the cells split for proliferation, soft agar assays. Cells were stained with trypan blue and counted using a hemocytometer to assay proliferation. For soft agar, 0.6% agar was used as the base layer and 0.5% agar as the top layer. The plates were counted manually using ImageJ (NIH). Apoptosis was assessed using the Annexin V-Cy3 Apoptosis Detection Kit (Sigma-Aldrich) according to the manufacturer's protocol. Flow cytometry was performed using the CyAn ADP (Beckman-Coulter). For assessment of autophagy, three days after lentiviral transduction A673 and EWS502 cells were split 1:3 and treated with 20 μM chloroquine for 3 hours or chloroquine followed by 10 ng/mL temsirolimus (LC Laboratories) for 20 hrs. Cells were lysed in CHAPS buffer and extracts were separated by SDS-PAGE.

IGF-1 inhibition

Cells were treated with NVP-AEW541 (Cayman Chemical) and OSI-906 (ChemieTek) at the indicated concentrations. Prior to treatment with IGF-1, cells were kept in serum-free media for two hours in combination with the IGF-1 inhibitor. Cells were then treated with IGF-1 (Cell Signaling Technologies) for 15 min and lysed in RIPA buffer (25 mM Tris-HCl pH 7.6, 150 mM NaCl, 1% NP-40, 0.1% SDS) supplemented with 200 mM $NaVO_4$ and 50 mM NaF. Cell extracts were separated by SDS-PAGE and blotted with anti-phospho AKT and imaged (LiCor). For assessment of cell viability, EWS502 cells were transduced with lentiviral pLL5.0-PTEN or pLL5.0 as a vector control. 24 hours post infection the cells were treated with NVP-AEW541 in complete media. Viability was assayed 72 hours following NVP-AEW541 treatment using WST-1 (Roche).

Tissue microarray (TMA) and Cell Line Array (CLA) construction

Pellets from the Ewing sarcoma cell lines were fixed in 10% buffered formalin (SF98-4, Fisher Scientific) for 16-24 hours, washed twice in 70% ethanol, clotted in 2% low-melting agarose (Fisher), and then embedded in paraffin wax. Blocks were sectioned and stained with hematoxylin and eosin (H&E, Hematoxylin 7211, Eosin 7111, Richard-Allan). Three 1 mm cores were removed and embedded into recipient CLA block. For TMA construction, Ewing sarcoma cases (n = 25) and controls (breast carcinoma, and PTEN-deleted sarcoma) were selected from The University of North Carolina Surgical Pathology and St. Jude Children's Research Hospital archives under an IRB-approved protocol. Hematoxylin and eosin (H&E) stained slides were re-reviewed and representative areas of tumor were marked for coring. TMA blocks, containing triplicate 0.6 mm cores per case were constructed. TMA and CLA blocks were cut into 4 and 5 micron sections respectively and placed on positively charged glass slides.

Immunohistochemistry (IHC) and Immunofluorescence (IF)

TMA and CLA slides were stained with CD99 and PTEN antibodies (Bond fully-automated slide staining system, Leica Microsystems). Slides were deparaffinized (Bond, AR9222) and hydrated in wash solution (Bond, AR9590). Epitope retrieval (pH 9.0, AR9640, Bond) was performed followed by a peroxide blocking step (Bond DS9800). CD99 and PTEN (1:400) antibodies were incubated for 15 and 30 minutes, respectively then secondary antibody was

applied (polymer, Bond DS9800). Chromogenic detection with 3,3'-diaminobenzidine (DAB) and hematoxylin was performed (Polymer Refine Detection, DS9800, Bond). Stained slides were dehydrated and mounted. For fluorescent detection, the TSA-Cy5 reagent (PerkinElmer), Hoechst 33258 (Invitrogen) and ProLong Gold antifade reagent (Molecular Probes) were used.

Imaging and digital image analysis

IHC stained TMA sections were digitally imaged (Aperio ScanScope XT, Aperio Technologies). High-resolution DAPI and Cy5 IF images were obtained (Aperio ScanScope FL). For digital images from IHC slides, Aperio's Cytoplasmic algorithm was used to determine the percentage and intensity of cells positive for PTEN or CD99. A PTEN-deleted tumor control was used to set the negative/low positive intensity threshold for the PTEN stained TMA slide. IF signal was quantified (Definiens Tissue Studio, version 3.6).

Results

A subset of Ewing Sarcomas lack PTEN

We recently reported widespread alterations in chromatin structure and histone modifications in Ewing sarcoma cells using high-throughput sequencing (5). Although the experiments performed were intended to detect nucleosome-depleted regions of chromatin, background signal from Formaldehyde Assisted Isolation of Regulatory Elements (FAIRE-seq) typically covers the remainder of the genome mappable by short sequencing read and thus offers a genome-wide sampling of DNA content. Unexpectedly, we observed an approximately 1 Mb region on chromosome 10 that demonstrated a nearly complete loss of FAIRE-seq signal, which we hypothesized to indicate homozygous deletion (Fig. 1A). The potential deletion encompassed several genes including the terminal exons of *PTEN* (Fig. 1A).

Since deletion of *PTEN* had yet to be detected in Ewing sarcoma using high throughput sequencing approaches, we verified this deletion by fluorescence *in situ* hybridization (FISH) using two probes that overlap the PTEN locus, as well as a control centromeric probe. One probe (G17) is fully contained within the deleted region whereas half of the second probe (D9) was predicted to hybridize outside the deletion (Fig. 1A). Probes were hybridized to seven Ewing sarcoma cell lines (EWS502, EWS894, A673, MHH-ES-1, SK-ES, RD-ES-1, SK-N-MC) and one control cell line (HUVEC). The absence of signal from the G17 probe in EWS502 cells confirmed a homozygous deletion at this region (Fig. 1B). Signal from the D9 probe was detected which likely results from hybridization to the retained region centromeric to the deletion. Signal was observed for both probes in the other Ewing sarcoma and control cell lines. However, EWS894 and SK-N-MC cells exhibited PTEN/centromeric probe ratios not equal to one suggesting other cytogenetic aberrations involving the long arm or centromere of chromosome 10 (Fig. 1B, C). EWS894 had two copies of the PTEN locus but three copies of the centromeric probe whereas one copy of the PTEN locus and two copies of the centromeric probe were detected in SK-N-MC. The PTEN/centromeric probe ratio was equivalent for the remaining cell lines; MHH-ES-1 and RD-ES exhibited triploidy of chromosome 10 (Sup. Fig. 1). Consistent with PTEN

chromosomal loss, PTEN protein was absent in EWS502 whereas other Ewing sarcoma cell lines showed variable levels (Fig. 1D).

In order to address whether PTEN was similarly lost in primary Ewing sarcoma tumor, we generated a tissue microarray consisting of 25 tumors diagnosed as Ewing Sarcoma during clinical evaluation. The samples were re-reviewed prior to microarray generation, and tumor-specific regions were selected for core preparation. Each tumor was represented in triplicate at random positions on the array. Microarray sections were hybridized to both FISH probes. For the 20 tumors from which FISH signal was interpretable, homozygous loss was not observed however copy number varied across tumors (Sup. Fig 2). Since PTEN expression can be affected by mechanisms other than deletion, we analyzed PTEN protein levels by immunofluorescence (IF) and immunohistochemistry (IHC). A Ewing sarcoma cell line array was generated to validate antibody-mediated detection of PTEN. PTEN detection by IHC and IF on the cell line array quantitatively matched detection by Western blotting ($r^2 = 0.74$, Sup. Fig 3). Because of the diverse age of the samples that contributed to the primary tumor array and the evolving criteria for Ewing sarcoma diagnosis, we performed IHC and IF for CD99 as confirmation of diagnosis and as a quality control. IHC and IF for CD99 as well as PTEN were highly concordant (Sup. Fig 4). After eliminating CD99 negative tumors and those with poor staining 15 tumors remained. A wide range of PTEN expression was detected by IF among the Ewing sarcoma samples. Three tumors demonstrated significantly reduced signal when compared to a PTEN-expressing control breast carcinoma sample and a PTEN-deficient undifferentiated sarcoma (Fig. 2A). Histological examination suggested that non-tumor cells confounded accurate PTEN quantification. We attempted IF for CD99 to specifically identify tumor cells, but due to technical constraints co-staining of PTEN and CD99 was not possible. However, using CD99 IHC in adjacent sections, we confirmed the IF results. We observed that for one additional tumor (tumor 2, Fig. 2A and B) 55% of the cells did not demonstrate PTEN signal (Sup. Fig. 5). Remaining PTEN expression in this sample may be related to CD99-negative non-tumor cells or tumor heterogeneity (Fig. 2B). These data suggest that PTEN expression is reduced in approximately 25% (4 of 15) of Ewing sarcomas, and that the loss of PTEN is primarily through mechanisms other than large genomic losses. This observation is consistent with other tumors in which PTEN expression is lost due to gene silencing or focal deletions (32-35).

PTEN loss in Ewing sarcoma augments AKT signaling

To determine the effect of PTEN loss on AKT signaling across Ewing sarcoma cell lines we examined phosphorylation at S473 and T308. Phosphorylation of these sites is indicative of AKT activation (23, 24). Among the cell lines tested, EWS502 had the highest level of pAKT (Fig. 3A). Low levels of S473 phosphorylation was also observed in EWS894, SK-ES, and RD-ES-1 cells. T308 phosphorylation was limited to EWS502. PDK1-associated phosphorylation of T308 is associated with full AKT activation (36, 37) and was only observed in the absence of PTEN suggesting that AKT activation is augmented by PTEN loss. We then ectopically expressed PTEN in EWS502 cells to test the association between PTEN levels and activated AKT. Increasing PTEN was associated with a progressive decrease in pAKT at S473 and T308 (Fig. 3B) suggesting that AKT activation in EWS502 is due in part to PTEN deficiency. To test whether PTEN loss altered IGF-1 sensitivity, we

examined dose-dependent stimulation by IGF-1 under serum-free conditions. AKT demonstrated baseline phosphorylation in all Ewing sarcoma cell lines. IGF-1 stimulation resulted in further AKT activation. However, there was no difference in IGF-1 IC50 (Sup. Fig. 6). These data indicate that PTEN levels influence AKT activation but do not result in enhanced sensitivity to IGF-1.

The cellular effects of PTEN loss in Ewing sarcoma were examined by testing the effect of PTEN on cellular proliferation and anchorage-independent growth. PTEN was transduced into EWS502 cells and expression was confirmed by immunoblotting. PTEN expression resulted in significantly decreased cellular proliferation (Fig. 3C). To address whether the reduction in cell proliferation following PTEN expression could be attributed to increased apoptosis, we assayed annexin V reactivity by flow cytometry and observed a significant increase relative to control cells (Fig. 3D). We also observed a similar increase in cleaved PARP (Sup. Fig. 7). Anchorage-independent growth as assayed by colony formation in soft agar was also greatly diminished (Fig. 3E). Taken together, these data demonstrate that PTEN loss enhances cellular properties associated with transformation in Ewing sarcoma cells.

PTEN loss decreases sensitivity to IGF-1 inhibition

Since clinical trials of IGF-1-targeted inhibitors have demonstrated robust but limited patient responses, we asked whether PTEN loss might mitigate the effect of these compounds in Ewing sarcoma cells. Ewing sarcoma cells were treated with two IGF-1R inhibitors, NVP-AEW541 (38) and OSI-906 (39). NVP-AEW541 has been tested for Ewing sarcoma whereas OSI-906 is an investigational agent for a variety of cancers (15, 16, 39-42). Cells cultured in serum-free media were pretreated with these inhibitors prior to stimulation by IGF-1. PTEN loss was associated with increased IC50 to the IGF-1 inhibitors as measured by AKT activation (Fig. 4A). This differential sensitivity was detectable by phosphorylation at both S473 and T308. Interestingly, intermediate sensitivity to these inhibitors was observed for EWS894 and SK-ES, both of which demonstrated lower PTEN levels and detectable pAKT-S473.

We then examined the effect of PTEN expression on IGF-1R inhibition focusing on NVP-AEW541 due to its selectivity for IGF-1R (38). Transduced PTEN resulted in enhanced sensitivity for NVP-AEW541 with an IC50 approximating the other PTEN-expressing Ewing sarcoma cells (Fig. 4B). The enhanced sensitivity for NVP-AEW541 was associated with increased cellular toxicity (Fig. 4C). These data suggest that PTEN loss in Ewing sarcoma diminishes the efficacy of IGF-1R inhibitors on PI3K signaling as well as viability.

PTEN loss enhances response to temsirolimus

AKT signaling acts on the mTOR pathway to influence multiple cellular processes including autophagy (43, 44). In light of the emerging role of mTOR inhibition in Ewing sarcoma treatment, we examined the relationship between PTEN loss and autophagic response to the mTOR inhibitor, temsirolimus. Ewing sarcoma cells were treated with temsirolimus and autophagy was assayed by quantification of LC3BII, a protein localized to autophagosome membranes that is generated during autophagy (45). The assay was performed in the

presence of chloroquine to inhibit lysosomal processing and thus enable assessment of autophagy without ongoing degradation. PTEN-expressing Ewing sarcoma cells (A673) demonstrated minimal LC3BII induction in response to chloroquine or to chloroquine and temsirolimus (Fig. 5A). In contrast, EWS502 cells demonstrated a modest induction of LC3BII in response to chloroquine, but this response was significantly increased by temsirolimus (Fig. 5B). Since EWS502 but not A673 cells demonstrated induction of temsirolimus-induced autophagy, we examined the effect of modulating PTEN. Silencing PTEN in A673 cells augmented the autophagic response to temsirolimus whereas exogenous PTEN expression in EWS502 eliminated the effect of temsirolimus (but not chloroquine) (Fig. 5A, B). We then examined the effect of inhibiting autophagy with chloroquine on cellular viability. Interestingly, treatment with chloroquine attenuated the toxic effects of temsirolimus in the absence of PTEN but this difference was lost when PTEN was expressed. (Sup. Fig. 8). Together these experiments demonstrate that PTEN expression in Ewing sarcoma cells influences autophagic response to temsirolimus with PTEN loss associated with increased responsiveness to mTOR inhibition. Further, the induction of autophagy by temsirolimus is associated with decreased viability, suggesting that autophagy partially mediates the effects of temsirolimus.

Discussion

The unexpected identification of PTEN deletion in a Ewing Sarcoma cell line led us to explore the status of PTEN in primary tumors. Although we were unable to detect a similar deletion in other cell lines or a set of primary tumors using FISH, quantitative assessment of PTEN expression by IHC and IF suggested that approximately 25% of Ewing sarcoma tumors are PTEN deficient. Small deletions and other mutations undetectable by FISH, in addition to gene silencing, remain alterative mechanisms that result in PTEN loss in Ewing sarcoma. However, our observation of PTEN loss is consistent with a recent study that used high resolution SNP arrays to examine copy number variation in Ewing sarcoma and observed PTEN deletion in 14% of the tumors (46).

We found that PTEN deficiency leads to enhanced AKT activation associated with decreased apoptosis, increased proliferation, and anchorage-independent growth. Enhanced properties associated with cellular transformation in Ewing sarcoma could result in a more aggressive tumor phenotype. Intriguingly, ETS deregulation may cooperate with PTEN loss to accelerate tumorigenesis (47). Several lines of evidence indicate that mTOR contributes to PTEN-dependent negative feedback regulation of AKT (reviewed in (48) (49)). The loss of PTEN in Ewing sarcoma may be one mechanism mediating hyperactivation of AKT even in the absence of growth factors such as IGF-1. In addition to potentially contributing to a more transformed phenotype, hyperactivation of AKT may decrease sensitivity of Ewing sarcoma cells to chemotherapy (50, 51).

We have demonstrated that loss of PTEN decreases sensitivity to IGF-1R inhibition, as measured by AKT phosphorylation. Of the limited number of available cell lines tested, there were varying degrees of response to IGF-1R inhibition. An intermediate effect was seen in two cell lines with reduced PTEN expression and increased AKT phosphorylation.

These findings are consistent with a prior study demonstrating that PTEN silencing in cultured glioblastoma decreased response to NVP-AEW541 (52).

PTEN loss led to increased sensitivity to temsirolimus treatment as marked by the activation of autophagy. Autophagy is a metabolic recycling process in which cellular components are broken down in times of stress to maintain metabolic homeostasis. The role of autophagy in cancer is complex. Our results suggest that autophagy is required to mediate the cell viability effects of mTOR inhibition by temsirolimus. These data are in agreement with studies indicating that induction of excessive autophagy can lead to cell death (53, 54). mTOR inhibitors may constitute a promising therapeutic class for cancers lacking functional PTEN by inducing autophagy-mediated apoptosis.

PTEN deficiency renders cells less sensitive to IGF-1R inhibition but increases autophagic response to mTOR inhibition. The differential response to AKT/mTOR pathway manipulation has therapeutic implications. The promise of personalized therapy for cancer depends on the identification of genetic alterations in specific tumors. The limited efficacy of IGF-1R inhibition offers an opportunity for the application of relevant biomarkers. Our results indicate that loss of PTEN expression may diminish the therapeutic response of Ewing sarcoma to IGF-1R inhibitors. However, our study also suggests a reciprocal interaction between PI3K/AKT signaling and autophagy. Whereas PTEN loss decreased sensitivity to IGF-1R inhibition, it enhanced sensitivity to temsirolimus. These data suggest that patients who are unresponsive to IGF-1R inhibition may benefit from mTOR inactivation. The application of PTEN expression as a biomarker to future clinical trial would be needed to directly assess this possibility. Due to interactions between the IGF-1R and mTOR pathways, combination of IGF-1R- and mTOR-directed therapies are being evaluated in preclinical and early phase clinical trials with evidence of efficacy. (55-58). The ability to identify and apply relevant prognostic biomarkers during the selection of biologically active therapies may greatly increase the possibility of therapeutic benefit.

Supplementary Material

Refer to Web version on PubMed Central for supplementary material.

Acknowledgments

The authors thank Mervi Eeva, Stephanie Cohen, Nana Feinberg, and Michelle Mathews from the Tissue Processing Laboratory, which is supported in part by UNC Lineberger Comprehensive Cancer Center Core Support Grant (P30CA016086), for tissue microarray generation and immunostaining of tissues. Ewing sarcoma samples were a gift from T. Look. We thank William Kim and Sean Bailey for constructive input. We gratefully acknowledge support from the National Institutes of Health (CA100400 and CA166447), the Hyundai Hope on Wheels Foundation, the Wide Open Charitable Foundation, and the Corn-Hammond Fund for Pediatric Oncology (UNC).

Financial support

This work was supported in part by the NIH (CA100400, CA166447), the Hyundai Hope on Wheels Foundation, The Wide Open Charitable Foundation, and the Corn-Hammond Fund for Pediatric Oncology. The UNC Translational Pathology Laboratory is supported in part, by grants from the National Cancer Institute (CA016086) and the UNC University Cancer Research Fund (UCRF).

References

1. Sorensen PH, Lessnick SL, Lopez-Terrada D, Liu XF, Triche TJ, Denny CT. A second Ewing's sarcoma translocation, t(21;22), fuses the EWS gene to another ETS-family transcription factor, ERG. Nature genetics. 1994; 6:146–51. [PubMed: 8162068]
2. Delattre O, Zucman J, Plougastel B, Desmaze C, Melot T, Peter M, et al. Gene fusion with an ETS DNA-binding domain caused by chromosome translocation in human tumours. Nature. 1992; 359:162–5. [PubMed: 1522903]
3. Kinsey M, Smith R, Lessnick SL. NR0B1 is required for the oncogenic phenotype mediated by EWS/FLI in Ewing's sarcoma. Molecular cancer research : MCR. 2006; 4:851–9. [PubMed: 17114343]
4. Smith R, Owen LA, Trem DJ, Wong JS, Whangbo JS, Golub TR, et al. Expression profiling of EWS/FLI identifies NKX2.2 as a critical target gene in Ewing's sarcoma. Cancer cell. 2006; 9:405–16. [PubMed: 16697960]
5. Patel M, Simon JM, Iglesia MD, Wu SB, McFadden AW, Lieb JD, et al. Tumor-specific retargeting of an oncogenic transcription factor chimera results in dysregulation of chromatin and transcription. Genome Res. 2012; 22:259–70. [PubMed: 22086061]
6. Herrero-Martin D, Osuna D, Ordonez JL, Sevillano V, Martins AS, Mackintosh C, et al. Stable interference of EWS-FLI1 in an Ewing sarcoma cell line impairs IGF-1/IGF-1R signalling and reveals TOPK as a new target. British journal of cancer. 2009; 101:80–90. [PubMed: 19491900]
7. Riggi N, Cironi L, Provero P, Suva ML, Kaloulis K, Garcia-Echeverria C, et al. Development of Ewing's sarcoma from primary bone marrow-derived mesenchymal progenitor cells. Cancer research. 2005; 65:11459–68. [PubMed: 16357154]
8. Scotlandi K, Benini S, Sarti M, Serra M, Lollini PL, Maurici D, et al. Insulin-like growth factor I receptor-mediated circuit in Ewing's sarcoma/peripheral neuroectodermal tumor: a possible therapeutic target. Cancer research. 1996; 56:4570–4. [PubMed: 8840962]
9. Yee D, Favoni RE, Lebovic GS, Lombana F, Powell DR, Reynolds CP, et al. Insulin-like growth factor I expression by tumors of neuroectodermal origin with the t(11;22) chromosomal translocation. A potential autocrine growth factor. The Journal of clinical investigation. 1990; 86:1806–14. [PubMed: 2174908]
10. Scotlandi K, Benini S, Nanni P, Lollini PL, Nicoletti G, Landuzzi L, et al. Blockage of insulin-like growth factor-I receptor inhibits the growth of Ewing's sarcoma in athymic mice. Cancer research. 1998; 58:4127–31. [PubMed: 9751624]
11. van Valen F, Winkelmann W, Jurgens H. Type I and type II insulin-like growth factor receptors and their function in human Ewing's sarcoma cells. Journal of cancer research and clinical oncology. 1992; 118:269–75. [PubMed: 1315779]
12. Toretsky JA, Kalebic T, Blakesley V, LeRoith D, Helman LJ. The insulin-like growth factor-I receptor is required for EWS/FLI-1 transformation of fibroblasts. The Journal of biological chemistry. 1997; 272:30822–7. [PubMed: 9388225]
13. Yakar S, Rosen CJ, Beamer WG, Ackert-Bicknell CL, Wu Y, Liu JL, et al. Circulating levels of IGF-1 directly regulate bone growth and density. The Journal of clinical investigation. 2002; 110:771–81. [PubMed: 12235108]
14. Martins AS, Mackintosh C, Martin DH, Campos M, Hernandez T, Ordonez JL, et al. Insulin-like growth factor I receptor pathway inhibition by ADW742, alone or in combination with imatinib, doxorubicin, or vincristine, is a novel therapeutic approach in Ewing tumor. Clinical cancer research : an official journal of the American Association for Cancer Research. 2006; 12:3532–40. [PubMed: 16740780]
15. Scotlandi K, Manara MC, Nicoletti G, Lollini PL, Lukas S, Benini S, et al. Antitumor activity of the insulin-like growth factor-I receptor kinase inhibitor NVP-AEW541 in musculoskeletal tumors. Cancer Res. 2005; 65:3868–76. [PubMed: 15867386]
16. Manara MC, Landuzzi L, Nanni P, Nicoletti G, Zambelli D, Lollini PL, et al. Preclinical in vivo study of new insulin-like growth factor-I receptor--specific inhibitor in Ewing's sarcoma. Clinical cancer research : an official journal of the American Association for Cancer Research. 2007; 13:1322–30. [PubMed: 17317844]

17. Kolb EA, Gorlick R, Lock R, Carol H, Morton CL, Keir ST, et al. Initial testing (stage 1) of the IGF-1 receptor inhibitor BMS-754807 by the pediatric preclinical testing program. Pediatric blood & cancer. 2011; 56:595–603. [PubMed: 21298745]
18. Pappo AS, Patel SR, Crowley J, Reinke DK, Kuenkele KP, Chawla SP, et al. R1507, a monoclonal antibody to the insulin-like growth factor 1 receptor, in patients with recurrent or refractory Ewing sarcoma family of tumors: results of a phase II Sarcoma Alliance for Research through Collaboration study. Journal of clinical oncology : official journal of the American Society of Clinical Oncology. 2011; 29:4541–7. [PubMed: 22025149]
19. Juergens H, Daw NC, Geoerger B, Ferrari S, Villarroel M, Aerts I, et al. Preliminary efficacy of the anti-insulin-like growth factor type 1 receptor antibody figitumumab in patients with refractory Ewing sarcoma. Journal of clinical oncology : official journal of the American Society of Clinical Oncology. 2011; 29:4534–40. [PubMed: 22025154]
20. Malempati S, Weigel B, Ingle AM, Ahern CH, Carroll JM, Roberts CT, et al. Phase I/II trial and pharmacokinetic study of cixutumumab in pediatric patients with refractory solid tumors and Ewing sarcoma: a report from the Children's Oncology Group. Journal of clinical oncology : official journal of the American Society of Clinical Oncology. 2012; 30:256–62. [PubMed: 22184397]
21. O'Neill A, Shah N, Zitomersky N, Ladanyi M, Shukla N, Uren A, et al. Insulin-like growth factor 1 receptor as a therapeutic target in ewing sarcoma: lack of consistent upregulation or recurrent mutation and a review of the clinical trial literature. Sarcoma. 2013; 2013:450478. [PubMed: 23431249]
22. Shukla N, Schiffman J, Reed D, Davis IJ, Womer RB, Lessnick SL, et al. Biomarkers in Ewing Sarcoma: The Promise and Challenge of Personalized Medicine. A Report from the Children's Oncology Group. Front Oncol. 2013; 3:141.
23. Vivanco I, Sawyers CL. The phosphatidylinositol 3-Kinase AKT pathway in human cancer. Nat Rev Cancer. 2002; 2:489–501. [PubMed: 12094235]
24. Downward J. PI 3-kinase, Akt and cell survival. Semin Cell Dev Biol. 2004; 15:177–82. [PubMed: 15209377]
25. Maehama T, Dixon JE. The tumor suppressor, PTEN/MMAC1, dephosphorylates the lipid second messenger, phosphatidylinositol 3,4,5-trisphosphate. The Journal of biological chemistry. 1998; 273:13375–8. [PubMed: 9593664]
26. Depowski PL, Rosenthal SI, Ross JS. Loss of expression of the PTEN gene protein product is associated with poor outcome in breast cancer. Modern pathology : an official journal of the United States and Canadian Academy of Pathology, Inc. 2001; 14:672–6.
27. Hsu CP, Kao TY, Chang WL, Nieh S, Wang HL, Chung YC. Clinical significance of tumor suppressor PTEN in colorectal carcinoma. European journal of surgical oncology : the journal of the European Society of Surgical Oncology and the British Association of Surgical Oncology. 2011; 37:140–7.
28. Sircar K, Yoshimoto M, Monzon FA, Koumakpayi IH, Katz RL, Khanna A, et al. PTEN genomic deletion is associated with p-Akt and AR signalling in poorer outcome, hormone refractory prostate cancer. The Journal of pathology. 2009; 218:505–13. [PubMed: 19402094]
29. Li J, Yen C, Liaw D, Podsypanina K, Bose S, Wang SI, et al. PTEN, a putative protein tyrosine phosphatase gene mutated in human brain, breast, and prostate cancer. Science. 1997; 275:1943–7. [PubMed: 9072974]
30. Wang SI, Puc J, Li J, Bruce JN, Cairns P, Sidransky D, et al. Somatic mutations of PTEN in glioblastoma multiforme. Cancer research. 1997; 57:4183–6. [PubMed: 9331071]
31. Rubinson DA, Dillon CP, Kwiatkowski AV, Sievers C, Yang L, Kopinja J, et al. A lentivirus-based system to functionally silence genes in primary mammalian cells, stem cells and transgenic mice by RNA interference. Nat Genet. 2003; 33:401–6. [PubMed: 12590264]
32. Poliseno L, Salmena L, Riccardi L, Fornari A, Song MS, Hobbs RM, et al. Identification of the miR-106b~25 microRNA cluster as a proto-oncogenic PTEN-targeting intron that cooperates with its host gene MCM7 in transformation. Sci Signal. 2010; 3:ra29. [PubMed: 20388916]

33. Tay Y, Kats L, Salmena L, Weiss D, Tan SM, Ala U, et al. Coding-independent regulation of the tumor suppressor PTEN by competing endogenous mRNAs. Cell. 2011; 147:344–57. [PubMed: 22000013]
34. Konishi N, Nakamura M, Kishi M, Nishimine M, Ishida E, Shimada K. Heterogeneous methylation and deletion patterns of the INK4a/ARF locus within prostate carcinomas. Am J Pathol. 2002; 160:1207–14. [PubMed: 11943705]
35. Yamaguchi Y, Takabatake T, Kakinuma S, Amasaki Y, Nishimura M, Imaoka T, et al. Complicated biallelic inactivation of Pten in radiation-induced mouse thymic lymphomas. Mutat Res. 2010; 686:30–8. [PubMed: 20060398]
36. Chalhoub N, Zhu G, Zhu X, Baker SJ. Cell type specificity of PI3K signaling in Pdk1- and Pten-deficient brains. Genes Dev. 2009; 23:1619–24. [PubMed: 19605683]
37. Mora A, Komander D, van Aalten DM, Alessi DR. PDK1, the master regulator of AGC kinase signal transduction. Semin Cell Dev Biol. 2004; 15:161–70. [PubMed: 15209375]
38. Garcia-Echeverria C, Pearson MA, Marti A, Meyer T, Mestan J, Zimmermann J, et al. In vivo antitumor activity of NVP-AEW541-A novel, potent, and selective inhibitor of the IGF-IR kinase. Cancer cell. 2004; 5:231–9. [PubMed: 15050915]
39. Mulvihill MJ, Cooke A, Rosenfeld-Franklin M, Buck E, Foreman K, Landfair D, et al. Discovery of OSI-906: a selective and orally efficacious dual inhibitor of the IGF-1 receptor and insulin receptor. Future Med Chem. 2009; 1:1153–71. [PubMed: 21425998]
40. Kuhn DJ, Berkova Z, Jones RJ, Woessner R, Bjorklund CC, Ma W, et al. Targeting the insulin-like growth factor-1 receptor to overcome bortezomib resistance in preclinical models of multiple myeloma. Blood. 2012; 120:3260–70. [PubMed: 22932796]
41. Flanigan SA, Pitts TM, Newton TP, Kulikowski GN, Tan AC, McManus MC, et al. Overcoming IGF1R/IR Resistance through Inhibition of MEK Signaling in Colorectal Cancer Models. Clin Cancer Res. 2013
42. Kuijjer ML, Peterse EF, van den Akker BE, Briaire-de Bruijn IH, Serra M, Meza-Zepeda LA, et al. IR/IGF1R signaling as potential target for treatment of high-grade osteosarcoma. BMC Cancer. 2013; 13:245. [PubMed: 23688189]
43. Asnaghi L, Bruno P, Priulla M, Nicolin A. mTOR: a protein kinase switching between life and death. Pharmacol Res. 2004; 50:545–9. [PubMed: 15501691]
44. Yea SS, Fruman DA. Achieving cancer cell death with PI3K/mTOR-targeted therapies. Ann N Y Acad Sci. 2013; 1280:15–8. [PubMed: 23551096]
45. Kabeya Y, Mizushima N, Ueno T, Yamamoto A, Kirisako T, Noda T, et al. LC3, a mammalian homologue of yeast Apg8p, is localized in autophagosome membranes after processing. The EMBO journal. 2000; 19:5720–8. [PubMed: 11060023]
46. Lynn M, Wang Y, Slater J, Shah N, Conroy J, Ennis S, et al. High-resolution genome-wide copy-number analyses identify localized copy-number alterations in Ewing sarcoma. Diagn Mol Pathol. 2013; 22:76–84. [PubMed: 23628818]
47. Chen Y, Chi P, Rockowitz S, Iaquinta PJ, Shamu T, Shukla S, et al. ETS factors reprogram the androgen receptor cistrome and prime prostate tumorigenesis in response to PTEN loss. Nature medicine. 2013; 19:1023–9.
48. Guertin DA, Sabatini DM. Defining the role of mTOR in cancer. Cancer cell. 2007; 12:9–22. [PubMed: 17613433]
49. Nardella C, Chen Z, Salmena L, Carracedo A, Alimonti A, Egia A, et al. Aberrant Rheb-mediated mTORC1 activation and Pten haploinsufficiency are cooperative oncogenic events. Genes & development. 2008; 22:2172–7. [PubMed: 18708577]
50. Toretsky JA, Thakar M, Eskenazi AE, Frantz CN. Phosphoinositide 3-hydroxide kinase blockade enhances apoptosis in the Ewing's sarcoma family of tumors. Cancer research. 1999; 59:5745–50. [PubMed: 10582694]
51. Hofbauer S, Hamilton G, Theyer G, Wollmann K, Gabor F. Insulin-like growth factor-I-dependent growth and in vitro chemosensitivity of Ewing's sarcoma and peripheral primitive neuroectodermal tumour cell lines. European journal of cancer. 1993; 29A:241–5. [PubMed: 8380698]

52. Hagerstrand D, Lindh MB, Pena C, Garcia-Echeverria C, Nister M, Hofmann F, et al. PI3K/PTEN/Akt pathway status affects the sensitivity of high-grade glioma cell cultures to the insulin-like growth factor-1 receptor inhibitor NVP-AEW541. Neuro Oncol. 2010; 12:967–75. [PubMed: 20378689]

53. Kanzawa T, Zhang L, Xiao L, Germano IM, Kondo Y, Kondo S. Arsenic trioxide induces autophagic cell death in malignant glioma cells by upregulation of mitochondrial cell death protein BNIP3. Oncogene. 2005; 24:980–91. [PubMed: 15592527]

54. Turcotte S, Chan DA, Sutphin PD, Hay MP, Denny WA, Giaccia AJ. A molecule targeting VHL-deficient renal cell carcinoma that induces autophagy. Cancer cell. 2008; 14:90–102. [PubMed: 18598947]

55. Kolb EA, Gorlick R, Maris JM, Keir ST, Morton CL, Wu J, et al. Combination testing (Stage 2) of the Anti-IGF-1 receptor antibody IMC-A12 with rapamycin by the pediatric preclinical testing program. Pediatric blood & cancer. 2012; 58:729–35. [PubMed: 21630428]

56. Kurmasheva RT, Dudkin L, Billups C, Debelenko LV, Morton CL, Houghton PJ. The insulin-like growth factor-1 receptor-targeting antibody, CP-751,871, suppresses tumor-derived VEGF and synergizes with rapamycin in models of childhood sarcoma. Cancer research. 2009; 69:7662–71. [PubMed: 19789339]

57. Naing A, LoRusso P, Fu S, Hong DS, Anderson P, Benjamin RS, et al. Insulin growth factor-receptor (IGF-1R) antibody cixutumumab combined with the mTOR inhibitor temsirolimus in patients with refractory Ewing's sarcoma family tumors. Clinical cancer research : an official journal of the American Association for Cancer Research. 2012; 18:2625–31. [PubMed: 22465830]

58. Schwartz GK, Tap WD, Qin LX, Livingston MB, Undevia SD, Chmielowski B, et al. Cixutumumab and temsirolimus for patients with bone and soft-tissue sarcoma: a multicentre, open-label, phase 2 trial. The lancet oncology. 2013; 14:371–82. [PubMed: 23477833]

Implications

PTEN status in Ewing sarcoma affects cellular responses to IGF-1 and mTOR-directed therapy; thus, justifying its consideration as a biomarker in future clinical trials.

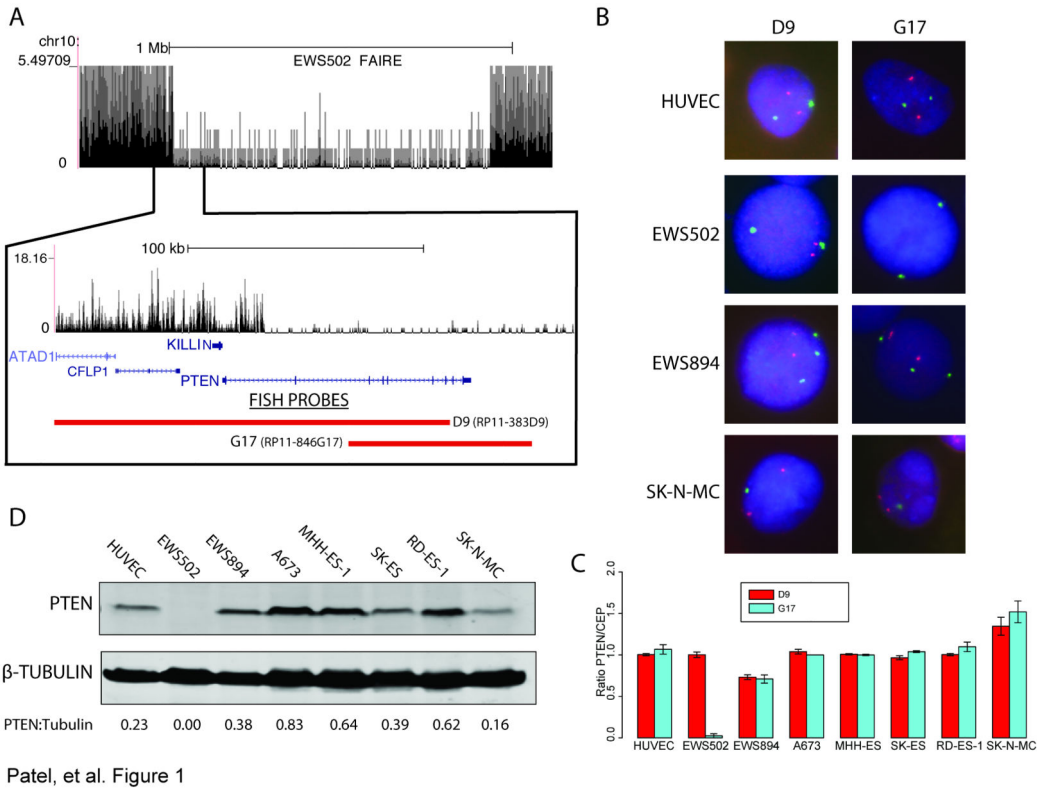

Figure 1. Identification of PTEN deletion in Ewing Sarcoma

A, FAIRE-seq derived high throughput sequencing tag density around the *PTEN* locus in EWS502. Red bars indicate the regions of hybridization for the FISH probes. Only genes located within the deletion are shown. B, *PTEN* FISH for representative Ewing sarcoma cell lines and a control (HUVEC). Chromosome 10 centromeric probe (green) and *PTEN* BAC probes (red) are shown. C, Observed ratio of PTEN probe to centromeric probe (CEP) signal. Error bars indicate standard deviation of PTEN/CEP probe ratio from five unique fields counting a minimum of 20 cells per field (with the exception of SK-ES in which 20 nuclei were analyzed). D, Immunoblot of PTEN in Ewing sarcoma cells. Extracts of EWS502, EWS894, A673, MHH-ES-1, SK-ES, RD-ES, and SK-N-MC and a control cell line, HUVEC were blotted with anti-PTEN antibody. Tubulin was used as a loading control.

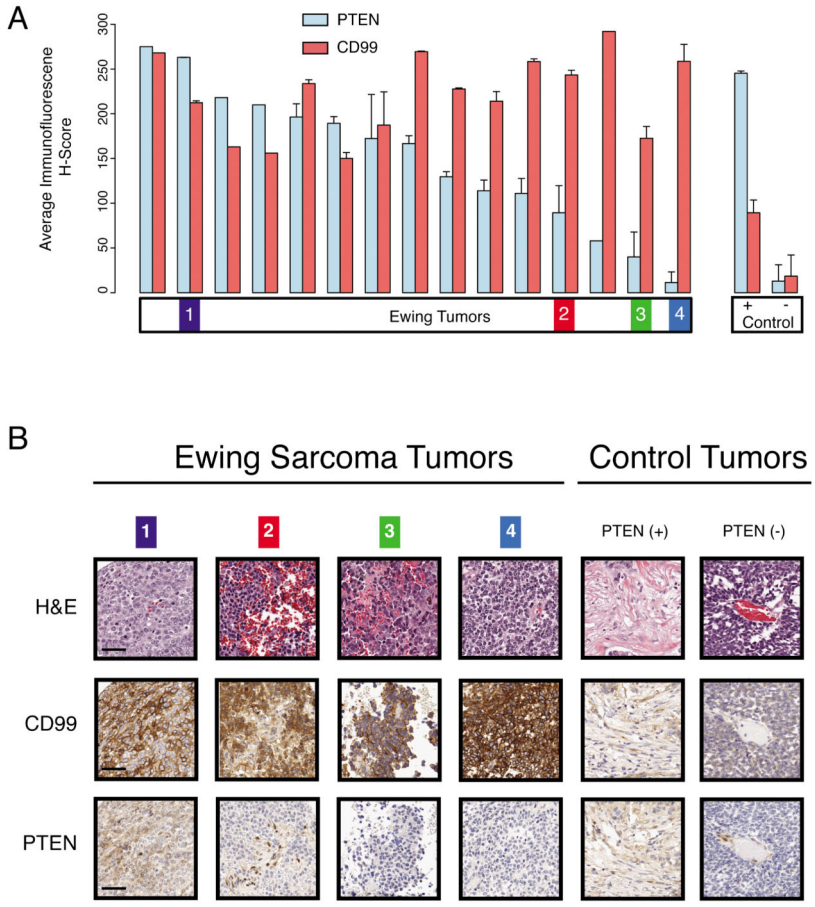

Figure 2. Loss of PTEN expression in primary Ewing Sarcoma

A, PTEN and CD99 immunofluorescence in Ewing sarcoma. Average immunofluorescence (H-score) for PTEN (blue bars) and CD99 (red bars) in Ewing sarcoma and control tumors. Positive (+) and negative (−) PTEN control tumors are shown to the right. Error bars represent standard deviation of H-scores between replicate cores. Absence of error bars indicates single core available for analysis. B, Representative hematoxylin and eosin (H&E), CD99, and PTEN diaminobenzidine (DAB) staining. Immunohistochemistry for selected Ewing sarcoma and control tumors (indicated in A) is shown. Scale bar, 50 μm.

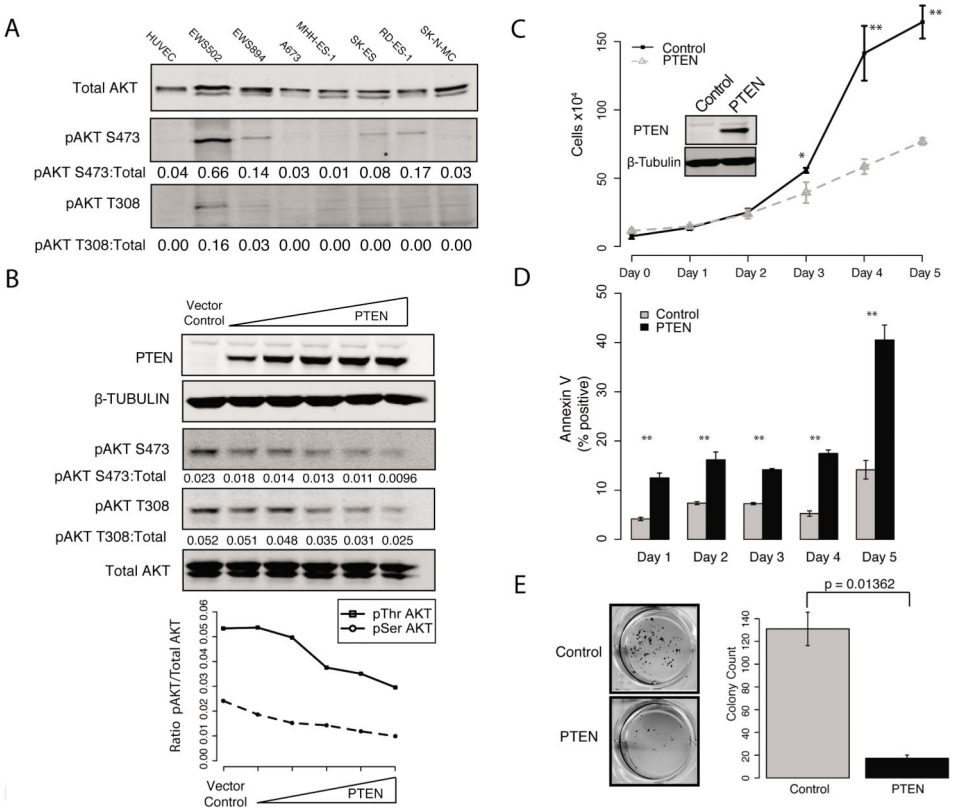

Figure 3. PTEN loss enhances AKT signaling promoting transformation

A, Immunoblot for total and phospho-AKT. Ewing cell lines and HUVEC under normal growth conditions were immunoblotted for phospho-AKT at S473 and T308. B, PTEN expression abrogates phospho-AKT. EWS502 were transduced with increasing amounts of PTEN-expressing lentivirus. Extracts were immunoblotted for PTEN, AKT, pAKT S473, pAKT T308, and tubulin. Phospho- and total AKT were quantified. The ratio of pAKT/AKT is shown (bottom). C, PTEN expression reduces cell proliferation. EWS502 were transduced with PTEN on day 0 and cells were counted daily. D, PTEN expression increases apoptosis. Annexin V staining in EWS502 cells transduced with PTEN (black) or a control vector (grey) were analyzed by flow cytometry. Percentages of annexin positive cells are shown. E, PTEN expression reduces colony formation. EWS502 transduced with PTEN or control vector were plated in soft agar. Colonies were stained with MTT for visualization (left) and quantified (right). Colonies greater than 1 mm in size were counted. For each panel, error bars represent standard error between triplicates. * and ** indicate $p < 0.05$ and $p < 0.01$ respectively (two-tailed T-test).

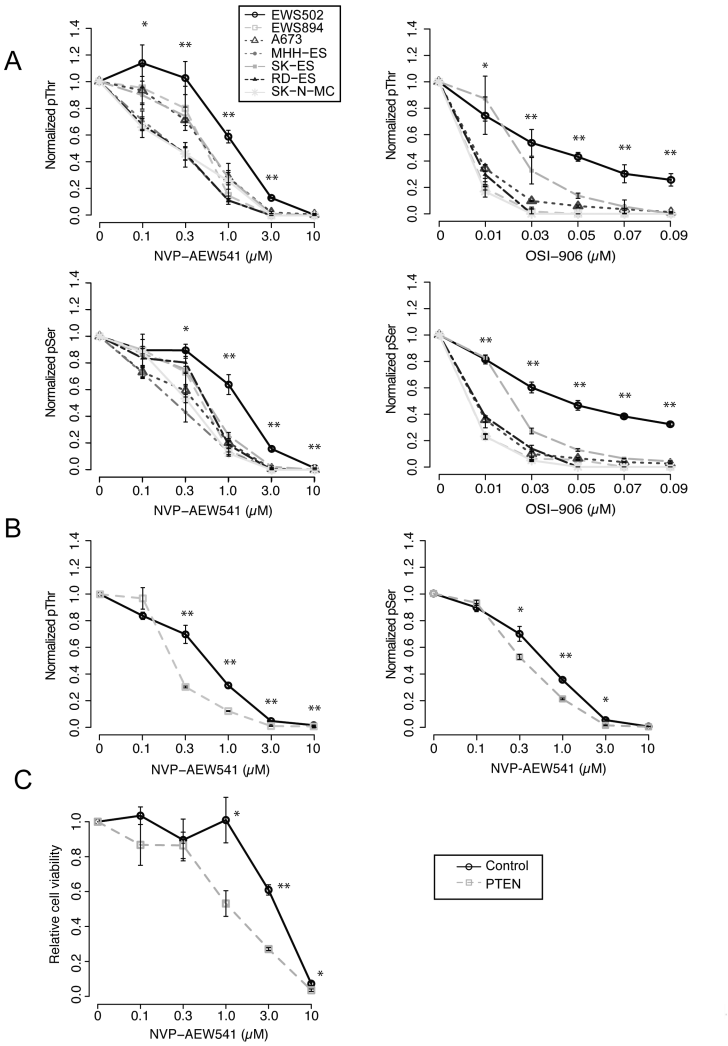

Figure 4. PTEN modulates sensitivity to IGF-1R inhibitors

A, PTEN loss decreases sensitivity to IGF-1R inhibitors. Ewing Sarcoma cells were treated with NVP-AEW541 (left) or OSI-906 (right) at the indicated concentrations for 2 hours in serum-free media and then stimulated with IGF-1 (5 ng/mL final concentration) for 15 min. Extracts were immunoblotted for pAKT at Thr 308 (top) and S473 (bottom) and results were quantified. Relative inhibition was calculated by normalizing pAKT signal to mock treatment (zero concentration). B, PTEN expression increases sensitivity to IGF-1R inhibition. EWS502 transduced with PTEN (dotted grey) or a control vector (solid black) were exposed to NVP-AEW541 for 2 hours in serum-free media and then stimulated with IGF-1 (5 ng/mL final concentration) for 15 min. Relative inhibition was calculated as above. C, PTEN expression increases the cellular toxicity associated with NVP-AEW541 treatment. EWS502 cells were transduced as in B and treated with NVP-AEW541 for 72 hours at indicated concentrations and assayed for viability. For each panel, error bars represent standard error between replicates. * and ** indicate $p < 0.05$ and $p < 0.01$ respectively (two-tailed T-test).

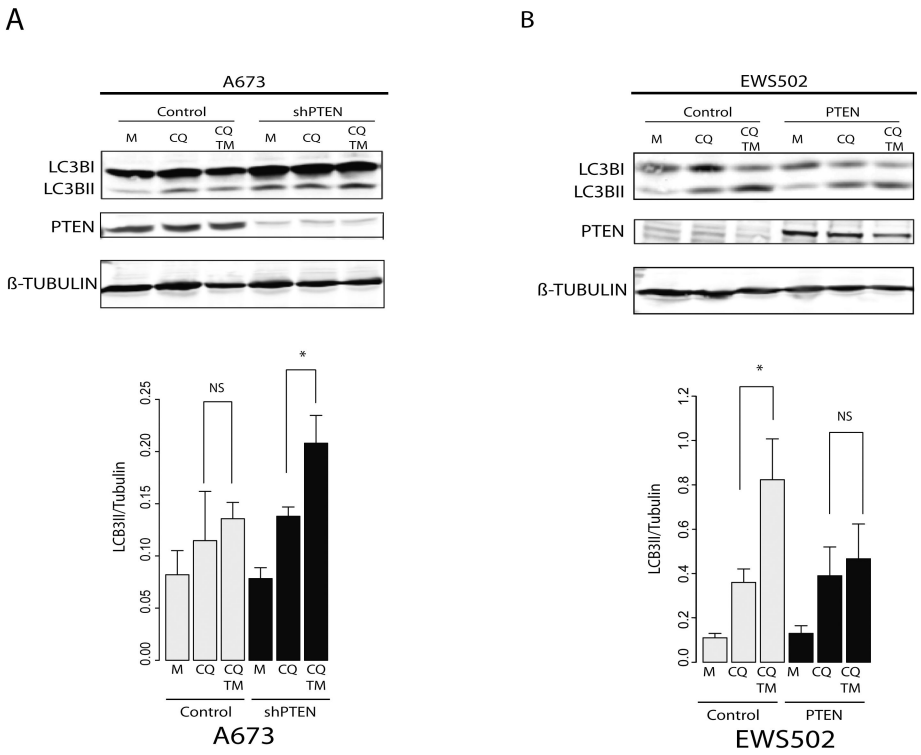

Figure 5. PTEN loss potentiates temsirolimus-induced autophagy

A, PTEN silencing enhances induction of autophagy in response to temsirolimus. A673 cells transduced with a PTEN-shRNA (shPTEN) or nonspecific control (shNS) were treated with chloroquine (CQ) alone or chloroquine and temsirolimus (10 ng/mL) for 20 hours (CQ/TM). Chloroquine was added 3 hours prior to the initiation of temsirolimus treatment. Cell extracts were immunoblotted for LC3B, PTEN, and tubulin (top). LC3BII bands were quantified and normalized to tubulin (bottom). B, PTEN expression abrogates induction of autophagy in response to temsirolimus treatment. EWS502 cells transduced with exogenous PTEN or a control vector (GFP) were treated with chloroquine (CQ) alone or chloroquine and temsirolimus (10 ng/mL) (CQ/TM) as described above. Cell extracts were immunoblotted and quantified as above. * and ** indicate $p < 0.05$ and $p < 0.01$ respectively by two-tailed T-test.